LIDAR SPATIAL RESOLUTION INTERPOLATION USING COLOR SIMILARITY OF OPTICAL IMAGE FOR ROAD SURFACE SURVEYING

Parawata Thanakitivirul , Sompong Liangrocapart , Suphongsa Khetkeeree, Chapkit Chansamorn

Mahanakorn University of Technology
140 Cheum-Sampan Rd., Nongchok, Bangkok, 10530, Thailand.
Email: kaero1999@hotmail.com ; sompong@mut.ac.th ; suphongs@mutacth.com ; chapkit@mut.ac.th

KEY WORDS: data fusion, road survey, road damage, DEM, bilateral filter

ABSTRACT The disadvantage of LiDAR sensor is lower spatial resolution than other sensors. Several data fusion techniques are employed to increase the information and the spatial resolution of the LiDAR sensor. Fortunately, the road surface surveying frequently has had optical image data. It is interesting to use this information to increase the LiDAR spatial resolution for reducing the expense. In this paper, we propose the interpolation algorithm to enhance the LiDAR spatial resolution for road surface surveying. It was formulated similar to the bilateral filter. By this algorithm, the color similarity of the correspondingly optical image data is employed to generate the interpolated LiDAR points. The results show that it can be used to analyze the road damage that cannot be identified by using a single video camera such as rutting, shoving, swell, etc.

1. INTRODUCTION

LiDAR sensor has been used to survey the building environment such as surface roads, railways or buildings because it can measure and collect data in three dimensions. Its data can create Digital Terrain Model (DTM) and Digital Elevation Model (DEM) of specific landscapes. Comparatively other sensors, the data got from LiDAR sensor has low spatial resolution. In the way to build up the better spatial resolution of LiDAR, the acquired point cloud must be post-processed by several techniques such as employ the internal information of LiDAR point or apply other information from any sensors. The overall process for obtaining the road surface information by using LiDAR sensor and optical image can be simply shown as Figure 1. Both sensors should be used to survey the road surface simultaneously because it will be convenient to fuse their data.

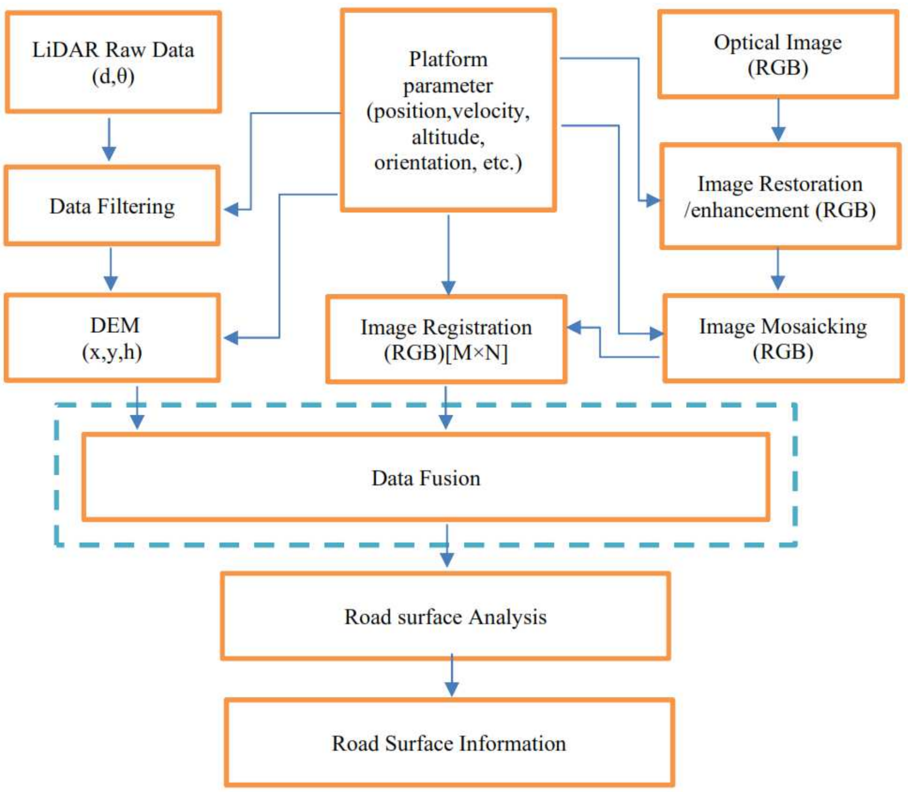

Figure 1. Overall process for obtaining the road surface information using the LiDAR sensor and the optical image.

Traditionally, the preprocess for correcting the unpleasant data each sensor is done. However, this process can be ignored if we have a high-performance sensor. After that, the point cloud data will be calculated to generate the road surface DEM. Then, the platform parameters such as the altitude, velocity, position and time stamp will be employed to register the corresponding position of the optical image. Due to the spatial resolution of the optical image often is higher than the LiDAR sensor. Thus, it is fascinating to use the optical image information in order to create a new spatial resolution of LiDAR. In this paper, we propose the interpolation algorithm for increasing the spatial resolution of road surface DEM. Our work is a part of a road surface survey and analysis that can be shown inside the dashed box in Figure 1. In this way, the pixel position and color similarity of the optical image data is used to be a reference for generating the interpolated DEM. As a result, the unidentified road damage such as rutting or shoving being hard to identify by a single 2D optical image can be seen by our process.

2. RELATED WORKS

2.1 Data fusion between LiDAR and optical image

The optical image is a popular one that frequently uses to increase the information of LiDAR data. Zhou et al. used the seamless fusion of the aerial image and the LiDAR data in order to extract the man-made building. By the aerial image, they created the aspects and aspects graph and merged them with the LiDAR data. The aspects and aspects graph were created from the aerial image. They merge the created aspects with the LiDAR data for building the geometric feature of the houses (Zhou et al., 2014). Lee et al. used multi-sensors such as the LiDAR, hyperspectral and photographic images, for monitoring the biodiversity and the structure of woodland. They proposed the technique based on the non-parametric image-registration techniques. The normalized gradient field and curvature were employed to design the regularization term (Lee et al., 2015). Xu et al. applied the data fusion between the terrestrial laser scanner (TLS) and the optical image on the Unmanned Aerial Vehicle (UAV) to reconstruct the cultural object. They employed the camera network to modify the image-based 3D reconstruction. This technique can be used to increase the image matching efficiency and reduce the mismatches (Xu et al., 2014). Zhou and Deng proposed the algorithm to establish the data association between the camera image and the 2-D LiDAR. The 2-D holography matrix was formulated based on non-linear optimization (Zhou and Deng, 2014).

2.2 Data interpolation

The interpolation is a method to construct the new data points within a range of a sampling data set. The fundamental techniques, i.e. nearest neighbor, linear, or cubic interpolation, are applied to many applications. Qu et al. (2013) applied the modified linear interpolation to improve the inaccuracy and edge blurring in image interpolation. The cubic interpolation was used to rescale the image in Sekar et al. works (Sekar et al., 2014). They applied this interpolation in the 2-D signal based on the Discrete Wavelet Transform (DTW). Such uncomplicated computational technique produces the smooth version of data interpolation. In our previous work, we proposed the non-linear interpolation based on the tetration polynomial. This work shows the behavior of non-symmetry and shift-variant properties (Khetkeeree and Chansamorn, 2019). Besides, several non-linear interpolation techniques based on the bilateral filtering were proposed in recent year, i.e. (Nair et al., 2019), (Ghosh et al., 2016) or (Chaudhurry and Dabhade, 2016). The advantage of the bilateral filter is that it can be used the information in a different domain to control the data filtering.

3. PROPOSED METHOD

In this section, we will present the approach of our interpolation formula and describe the interpolation algorithm to increase the spatial resolution of LiDAR DEM.

3.1 Interpolation Formula

We consider the color of the correspondingly optical image to determine the interpolated points of LiDAR point cloud of the road surface. We assume the area that has the same color should be had the same elevation. Most optical images are composed of three components as red, green and blue or RGB that it needs many ways of decisions to differentiate between RGB1 to RGB2. Hence, we transform the RGB image to panchromatic image by the following equation.

$$Pan(x,y) = 0.2126 \cdot R(x,y) + 0.7152 \cdot G(x,y) + 0.0722 \cdot B(x,y) \quad R,G,B \in [0,1] \tag{1}$$

But a panchromatic image may be transformed from many different RGB iamge. And from our observation, the green and blue color combination are more benefit than all combination (red, green and blue color) especially an asphalt road surface. Thus, we propose this color model for measuring the road surface color as

$$GB(x,y) = 0.5 \cdot G(x,y) + 0.5 \cdot B(x,y) \tag{2}$$

Where we called this equation (2) as "GB model". Figure 2 shows several road surfaces in three models as RGB, Panchromatic, and GB model included its histograms. GB model has more dynamic range than the panchromatic image.

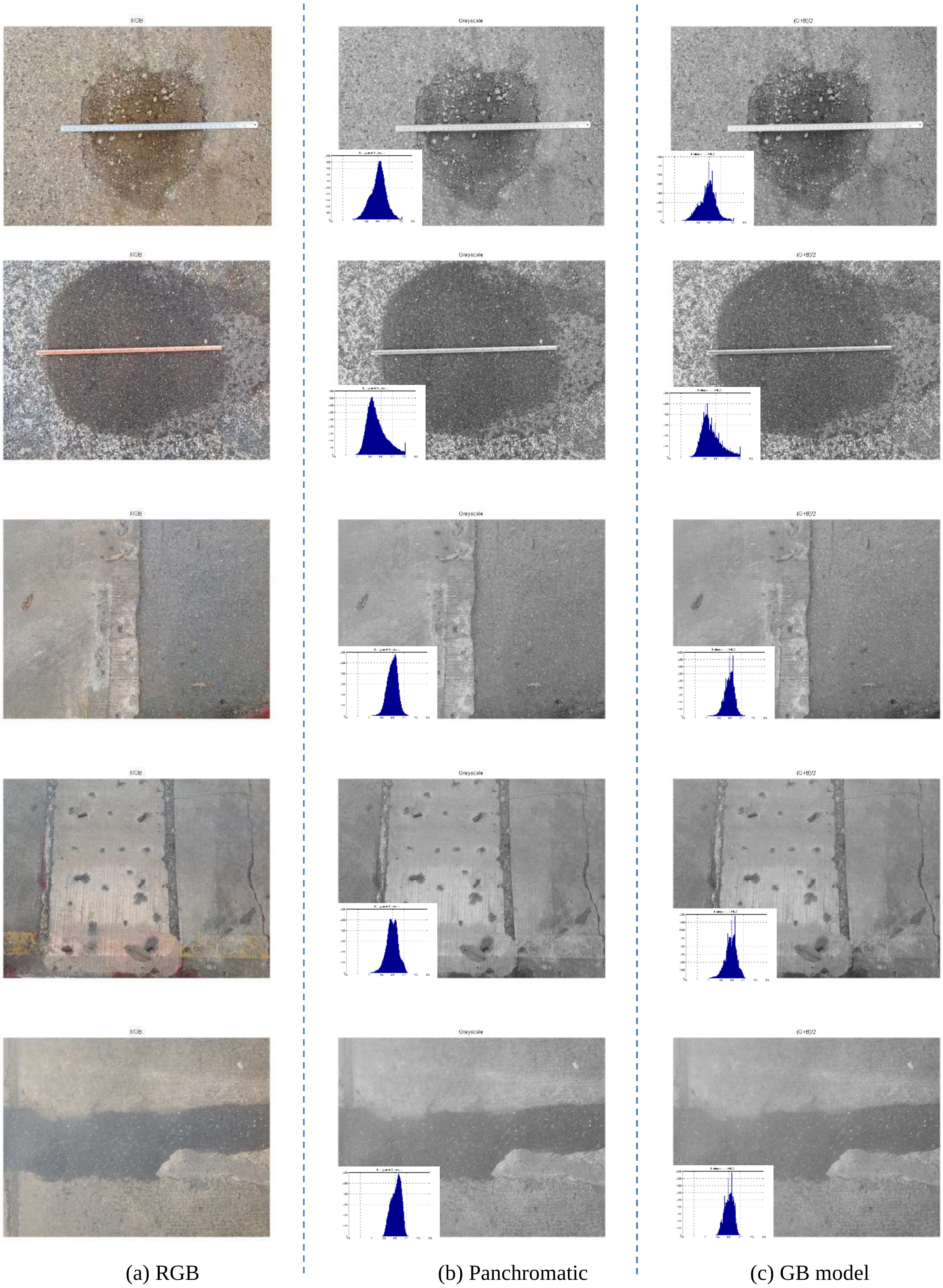

(a) RGB (b) Panchromatic (c) GB model

Figure 2. Visual and histogram comparison of road surface in (a) RGB color, (b) Panchromatic color and (c) GB model.

This property will be used to extract the area that has the same color. The GB model will be applied to determine the interpolate DEM point, and we use the Gaussian function to find the color similarity. The formula is constructed similar to the bilateral filter as the following equation.

$$D_{i,j}^{HR} = \frac{1}{K}\sum_{all} D_{k,l}^{LR} \cdot \exp\left[-\frac{\left\|\vec{r}_{i,j} - \vec{r}_{k,l}\right\|^2}{2\sigma_r^2}\right] \cdot \exp\left[-\frac{\left(GB_{i,j} - GB_{k,l}\right)^2}{2\sigma_{GB}^2}\right] \tag{3}$$

where

$$K = \sum_{all} \exp\left[-\frac{\left\|\vec{r}_{i,j} - \vec{r}_{k,l}\right\|^2}{2\sigma_r^2}\right] \cdot \exp\left[-\frac{\left(GB_{i,j} - GB_{k,l}\right)^2}{2\sigma_{GB}^2}\right] \tag{4}$$

where K is a normalized factor,
$D_{i,j}^{HR}$ is a high spatial resolution DEM (HR-DEM),
$D_{k,l}^{LR}$ is a low spatial resolution DEM (LR-DEM),
$\vec{r}$ is a position of the considered point,
GB is a grayscale level of the GB model,
σ_r is the span of local interpolation,
σ_{GB} is the span of color similarity comparison,
and the (i, j) and (k, l) is the position of the interpolated point and low spatial DEM.

3.2 Interpolation Process

Our proposed algorithm can be demonstrated in 1-D interpolation as Table 1. The first row represents the position of interest area. The second row represents the data of the RGB image in each position. Since our algorithm will be used to increase the spatial resolution up to the resolution of the RGB image. We desire HR-DEM in many positions since it was unknown so far. At the position where HR-DEM was unknown, the HR-DEM on that position will be assigned by our interpolation. The interpolation by the equation (3) can generate the desired HR-DEM. Such an assignment requires neighborhood LR-DEM and RGB. The bigger is the greater number of neighborhoods LR-DEM and RGB are calculated for interpolation. For the area that color does not change with position, the nearest LR-DEM has a higher influence than other LR-DEM to assign HR-DEM (by interpolation). For the different color area, the interpolated data will depend on both the distance and its RGB color when comparing with the LR-DEM.

Table 1. Interpolation algorithm for increasing the spatial resolution of 1-D DEM.

Position	1	2	3	4	5	6	7	8	9	10
RGB	●	●	●	●	●	●	●	●	●	●
LR-DEM	N/A	N/A	●	N/A	N/A	N/A	N/A	●	N/A	N/A
HR-DEM	I	I	A	I	I	I	I	A	I	I

● is a known data, N/A is an unknown data, I is an interpolated data, A is an actual data

4. SIMULATION RESULTS AND DISCUSSIONS

The experiments were divided into 2 sections. Firstly, the 1D simulation is presented to demonstrate the behavior of our proposed method. After that, the simulation results with the optical image of the actual road surface and corrected LiDAR point cloud was shown and described.

4.1 1D Simulation Test

Figure 3 shows the RGB, GB which generated from RGB and the generated of 1D HR-DEM. The RGB image is transformed into GB image. We can see that the violet band on the left and the dark blue on the right give the same GB appearance, but it is no effect to road surveying. The red circle is an actual point in 1D DEM and the blue star is an interpolated 1-D DEM which was calculated from (3).

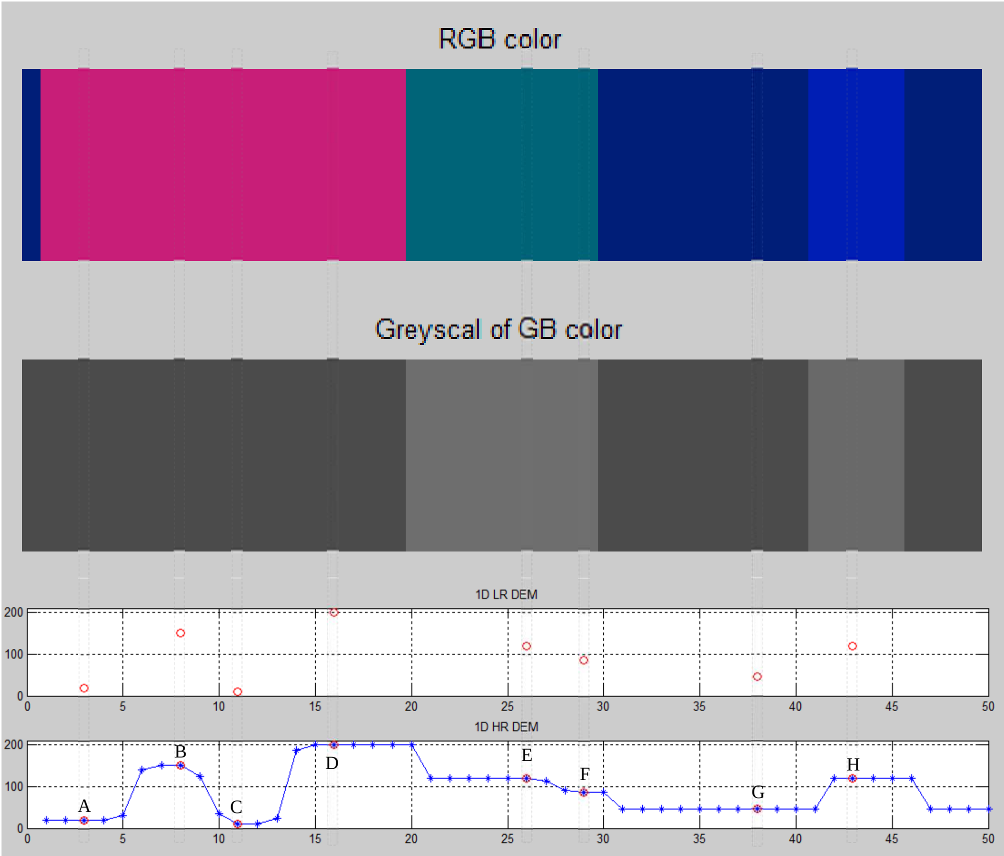

Figure 3. Illustrated the idea of 1D HR-DEM construction.

The LR-DEM points are represented by the red circles at point A, B, C, …, H and the HR-DEM points are represented by the blue stars. Figure 3 shows that the star height is interpolated by the height of the circle and color similarity of the GB model. At every star that has the same x value as a circle is calculated by equation (3), and its result approximates to the height of the circle. For the location of the stars with no corresponding circle, the height of these stars should change smoothly as the interpolation manner (see point A, B, and C). The nearest LR-DEM in the same color will more influence than others. We can see, the height of stars is dragged to the height of nearest LR-DEM (star point-between A to C). The special case is location between D and E, where the height of star changes abruptly from about x = 20 to x= 21. This abrupt change occurs when the GB scale change level at x = 20. The effect of LR-DEM will be depended on the color similarity. The height of star point between D and E is interpolated close to the same GB color LR-DEM.

4.2 Actual Road Surface Simulation

In this section, the actual road surface will be applied to demonstrate our algorithm. Figure 4 shows the results of each process in this demonstration. The optical image (RGB image) in figure 4 (a) is an interesting area image. Firstly, the actual positions associated with image pixel are calculated as the template positions. Next, the LR-DEM is filled in this template. We can see this result in Figure 4(b). In the third step, the GB image is processed as Figure 4 (c). From figure4 (c), the greyscale of the GB image is more contrast than the RGB image. In the next step, our algorithm is applied to increase the spatial resolution of LR-DEM as Figure 4 (d). We called the result in this step that HR-DEM. Now, the spatial resolution of HR-DEM is equal to the resolution of the referenced image. From figure 4 (d), we can see the pit in the HR-DEM which is clearer than the LR-DEM. In figure 4 (e) and 4 (f), we tried to mix the LR-DEM and HR-DEM with the corresponding terrestrial color. It helps us to see the pit detail very clear. In addition, we can use HR-DEM with the terrestrial color to exactly estimate the damage size of this road.

(a) RGB image

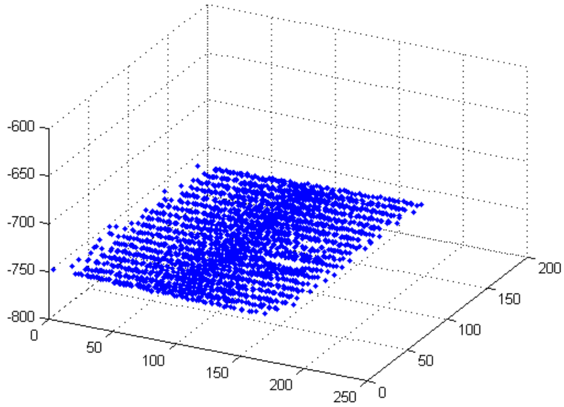

(b) LR-DEM

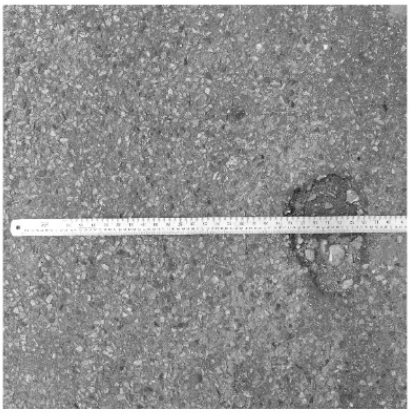

(c) GB image

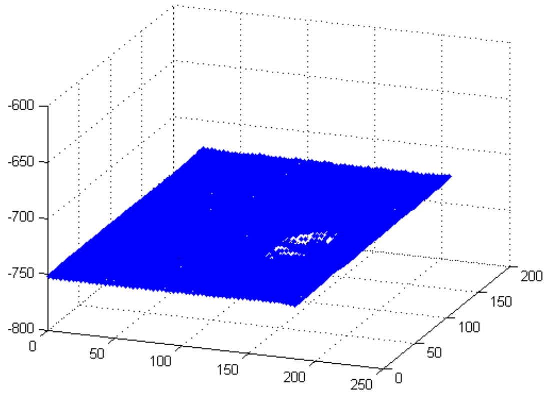

(d) HR-DEM

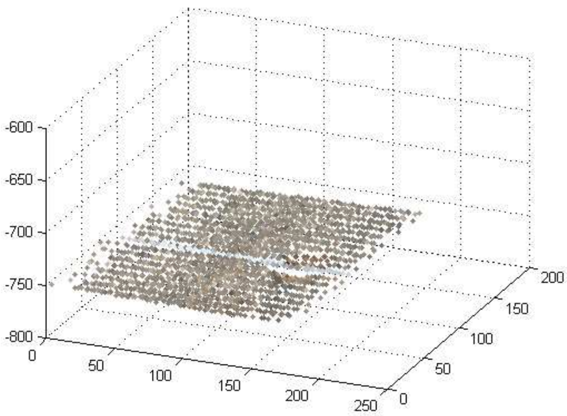

(e) LR-DEM with terrestial color

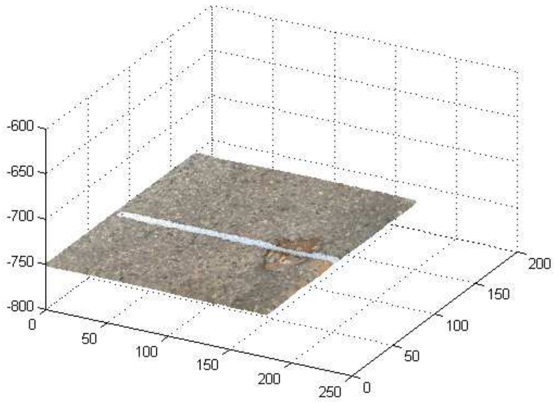

(f) HR-DEM with terrestial color

Figure 4. The actual road results of each process (a) RGB image, (b) LR-DEM, (c) GB image, (d) HR-DEM, (e) LR-DEM with terrestial color and (f) HR-DEM with terrestial color.

For another road damage, the depressed surface is considered as Figure 5 (a). In this image, the road surface is repaired by uncompressed asphalt. The results of LR-DEM with terrestrial color is shown in Figure 5 (b) and the HR-DEMs with terrestrial color in different viewpoints are demonstrated in Figure 5 (c) – (e). Figure 5 (f) is the image of HR-DEM with height level color. We can see that the height of HR-DEM in the damaged area smoothly deceased to the bottom of the depressed surface. From these experiments, it implies that the other road damage such as rutting, shoving and swell can be properly measured.

(a) RGB image

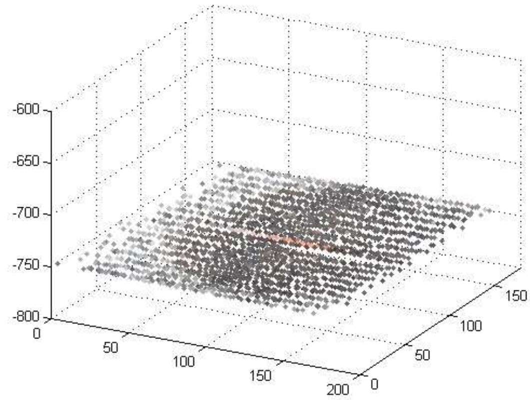

(b) LR-DEM with terrestrial color

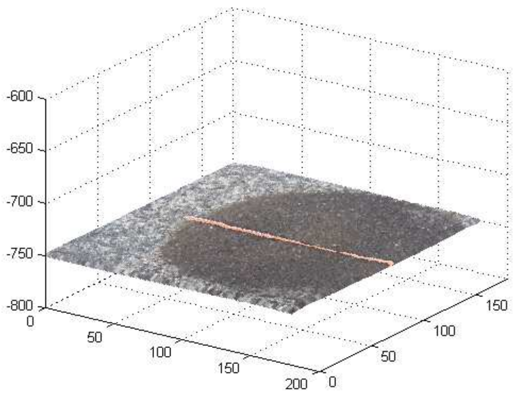

(c) HR-DEM with terrestial color (1)

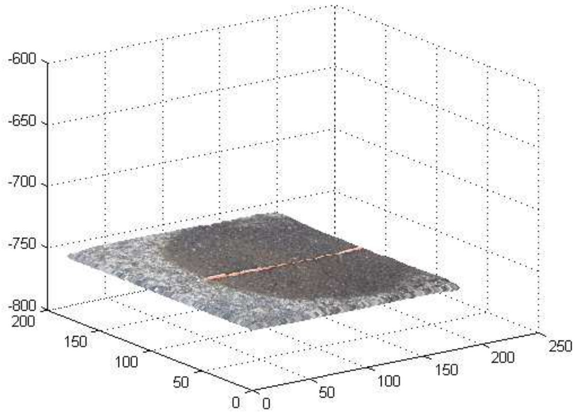

(d) HR-DEM with terrestial color (2)

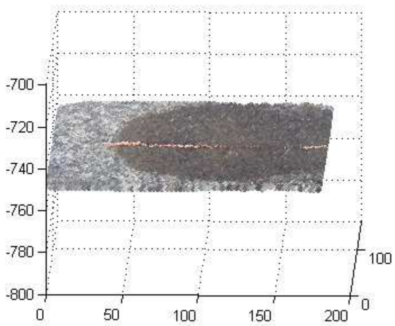

(e) HR-DEM with terrestial color (3)

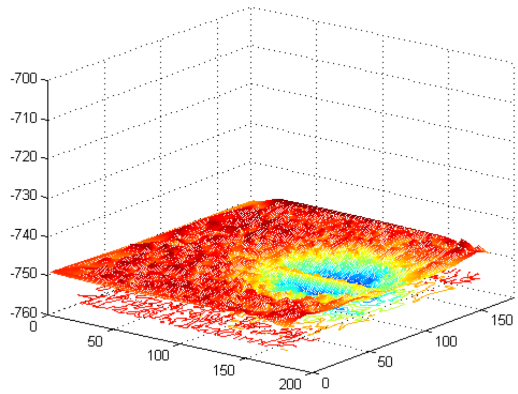

(f) HR-DEM with Height level color

Figure 5. The example of the depressed surface. (a) RGB image, (b) LR-DEM with terrestrial color, (c) HR-DEM with terrestial color (1), (d) HR-DEM with terrestial color (2), (e) HR-DEM with terrestial color (3), and (f) HR-DEM with height level color.

5. CONCLUSIONS

In this paper, the technique to interpolate the LiDAR DEM was proposed. The color similarity of the correspondingly optical image was employed to consider the weighting effect from actual LiDAR point. The GB image was proposed to apply in our formula because the road surface has nearly color. The bilateral filter based on the Gaussian function was applied to build our formula. The results show that our algorithm can be used to generate the high spatial resolution DEM of the road surface. This resolution is depended on the resolution of the optical image. The HR-DEM with terrestrial color was very clear and It can be used to analyze the road damage in both 2-D and 3-D viewpoint. Therefore, the similar road damage, i.e. rutting, shoving or swell, can be properly detected by our technique.

REFERENCES

Chaudhurry, K.N. and Dabhade, S.D., 2016. Fast and provably accurate Bilateral Filtering. In: IEEE Transaction on Image Processing, 25(6), June 2016, pp. 2519-2528.

Ghosh, S. and Chaudhury, K.N., 2018. Color Bilateral Filtering using Stratified Fourier Sampling. In: IEEE Global Conference on Signal Information Processing, November 2018.

Khetkeeree, S. and Chansamorn, C., 2019. Signal Reconstruction using Second Order Tetration Polynomial. International Technical Conference on Circuits/System, Computer and Communications, Jeju, South Korea, June 23-26, pp. 384-387.

Lee, J., Cai, X., Schonlieb, C.B., and Coomes, D.A., 2015. Nonparametric Image Registration of Airborne LiDAR, Hyperspectral and Photographic Imagery of Wooded Landscapes. IEEE Transactions on Geoscience and Remote Sensing, 53(11), November, 2015.

Nair, P. and Chaudhury, K.N., 2019. Fast High-Dimensional Bilateral and Nonlocal Means Filtering. IEEE Transactions on Image Processing, 28(3), March 2019, pp. 1470-1481.

Qu, Z., Yang, Y., and Wang, R., 2013. Linear Interpolation with Edge-preserving Adaptive Weights. 6th International Congress on Image and Signal Processing (CISP), Hangzhou, China, December 16-18.

Sekar, K., Duraisamy, V. and Remimal, A.M., 2014. An Approach of Image Scaling using DWT and Bicubic interpolation. International Conferrence on Green Computing Communication and Electrical Engineering, Coimbatore, India, March 6-8.

Xu, Z., Wu, L., Shen, Y., Li, F., Wang, Q. and Wang, R., 2014. Tridimensional Reconstruction Applied to Cultural Heritage with the Use of Camera-Equipped UAV and Terrestrial Laser Scanner. Remote Sensing, 6, pp. 10413-10434.

Zhou, G. and Zhou, X., 2014. Seamless Fusion of LiDAR and Aerial Imagery for Building Extraction. IEEE Transactions on Geoscience and Remote Sensing, 52(11), November, 2014.

Zhou, L. and Deng, Z., 2014. A New Algorithm for the Establishing Data Association between a Camera and a 2-D LiDAR. Tsinghua Science and Technology, 19(3), pp. 314-322.